Eurographics Workshop on Visual Computing for Biology and Medicine (2012)
T. Ropinski, A. Ynnerman, C. Botha, and J. Roerdink (Editors)

Deriving and Visualizing Uncertainty in Kinetic PET Modeling

Khoa Tan Nguyen[1] and Alexander Bock[1] and Anders Ynnerman[1] and Timo Ropinski[1]

[1]Linköping University, Sweden

Abstract

Kinetic modeling is the tool of choice when developing new positron emission tomography (PET) tracers for quantitative functional analysis. Several approaches are widely used to facilitate this process. While all these approaches are inherently different, they are still subject to uncertainty arising from various stages of the modeling process. In this paper we propose a novel approach for deriving and visualizing uncertainty in kinetic PET modeling. We distinguish between intra- and inter-model uncertainties. While intra-model uncertainty allows us to derive uncertainty based on a single modeling approach, inter-model uncertainty arises from the differences of the results of different approaches. To derive intra-model uncertainty we exploit the covariance matrix analysis. The inter-model uncertainty is derived by comparing the outcome of three standard kinetic PET modeling approaches. We derive and visualize this uncertainty to exploit it as a basis for changing model input parameters with the ultimate goal to reduce the modeling uncertainty and thus obtain a more realistic model of the tracer under investigation. To support this uncertainty reduction process, we visually link abstract and spatial data by introducing a novel visualization approach based on the ThemeRiver *metaphor, which has been modified to support the uncertainty-aware visualization of parameter changes between spatial locations. We have investigated the benefits of the presented concepts by conducting an evaluation with domain experts.*

1. Introduction

Positron emission tomography (PET) is one of the most widely used functional imaging modalities and it is applied in medical research as well as during everyday diagnosis. Depending on the chosen tracer injected into a subject, PET can be used, for instance, to visualize the brain activity or to assess the impact of a cardiovascular event by enabling the analysis of the myocardium vitality. In a typical PET study, PET data is obtained over a period of time and is composed of various signals that represent the tracer concentration for each time step. Kinetic PET modeling is based on mathematical models that enable isolating those components of the signal which are of interest. By applying this model analysis it becomes possible to understand the physiology and the pathophysiology of metabolism. Thus kinetic PET modeling paves the way for quantified PET analysis which enables comparative studies and researching the correlation between PET uptake and signals obtained from other modalities. Unfortunately the modeling process itself is tedious and time-consuming. Although the costs for developing a new tracer are in general lower than the costs for developing a new drug, the fact that 39% of new drug candidates fail due to inadequate pharmacokinetics [Wal04] suggests that effective modeling approaches are of great interest.

Like many other disciplines of medical research, kinetic PET modeling nowadays is performed with dedicated application packages [CHP81, BBC*98, BB97, MC01]. The current practice is, however, to chose one modeling approach early on in the analysis process as the different kinetic modeling approaches are supported as separate features. In this paper, we propose to assess the standard kinetic PET modeling approaches in an integrated manner in order to improve the modeling result. This allows us to derive inter-model uncertainty which is based on the different results of the standard modeling approaches. We further derive intra-model uncertainty, based on a single modeling approach, which is visualized in an integrated manner together with the inter-model uncertainty. To further facilitate the user in reducing the modeling uncertainties, we propose a visualization metaphor that is based on the *ThemeRiver* metaphor [HHN00], and takes into account the spatial and temporal properties of the kinetic PET modeling process. By enabling to relate the kinetic modeling parameters with each other this metaphor bridges the

gap between the different modeling approaches. Thus the main contributions of this paper are:

- Intra- and inter-model uncertainty derivation based on standard kinetic PET modeling approaches.
- Integrated visualization of micro and macro parameter uncertainty to combine and compare the results of standard kinetic PET modeling approaches.

The paper is structured as follows. In Section 2 we review the related work covering modeling systems and visualization techniques. In Section 3 we provide necessary background for readers, who are not familiar with kinetic PET modeling. The derivation of uncertainty is presented in Section 4. In Section 5 we describe in detail the proposed uncertainty-aware visualization technique as well as the design decisions for the integrated visualization of micro and macro parameter uncertainty. Section 6 presents the evaluation and the feedback of domain experts. The paper concludes in Section 7.

2. Related Work

2.1. Visualization Techniques

In the last years several general visualization techniques allowing representation of time-varying data sets have been proposed. A thorough review of the field would be beyond the scope of this paper, we refer to the survey presented by Aigner et al. [AMM*08] and focus on those techniques directly related to our approach. In addition, we also refer to [PWL97, JS03] for more detail information on different uncertainty visualization techniques for volumetric data sets. The most basic techniques for time-varying data, i. e., line graphs or sequence charts, are in fact several hundred years old [MMHE11]. While most of the views incorporated in our visualization can be considered as standard visual representations, we also propose a novel view linking abstract and spatial representations. This view is based on the *ThemeRiver* visualization metaphor [HHN00] which has been originally proposed to visualize variations over time in document collections. The metaphor is similar in spirit to line charts but allows a better correlation with external events. In contrast with the extension we propose in this paper the original metaphor does not allow to be linked to spatial entities. The same is true for the widely used parallel coordinate display [Ins85]. Huaiqing et al. [HLX11] showed that it is possible to include an uncertainty visualization into both parallel coordinates and star glyphs by introducing an additional dimension to the respective plot. Recently Malik et al. [MMHE11] proposed a visual analytics system that allows exploration of time correlations by taking into account a spatial component. While this system puts more emphasis on abstract data, related work more targeted towards scientific visualization also exists. Oeltze et al. [ODH*07] presented an interactive visual analysis approach for the evaluation of perfusion data. The authors employed multiple views for high dimensional data visualization and combined statistics with brushing and linking for the analysis of diffusion data. A more general approach for integrating abstract and spatial data has been proposed by Balabanian et al. [BYV*08, BVG10]. They integrate renderings of subvolumes of interest into a hierarchy visualization derived from the same data. Thus, they are able to show the components of a complex system in its hierarchical context. While this approach also targets towards the integration of abstract and spatial representations, it differs from our approach in a sense that the temporal component was not considered.

2.2. Kinetic Modeling Systems

There are several software packages supporting the kinetic PET modeling process, e. g., *KMZ* [BB97], *BLD* [CHP81], *SAAM/SAAM II* [BBC*98], and *PMOD* (PMOD Technologies Ltd., Zurich, Switzerland). The *KMZ* system separates the graphical user interface and the numerical calculation unit for extensibility. This system is, however, limited to the application of a rather low number of pre-defined kinetic model structures, and does not support model analysis and parameter modification as an integral part. *PMOD* is a flexible successor of *KMZ* and commercially available on various platforms. This software package allows different types of modeling, e. g., general kinetic modeling or pixel-wise modeling. It also supports image fusion and surface-based volumetric data visualization. Muzic et al. [MC01] have proposed another flexible PET compartmental modeling framework named *COMKAT*. It provides the ability to implement arbitrary user-specified models through graphical and command-line interaction. *KIS* system [HTW*05] is an Internet-based kinetic imaging system for microPET. In comparison with other existing software systems, *KIS* incorporates an educational aspect aiding users in better understanding the modeling process. Even though this package was initially designed for microPET only its design allows handling general imaging studies in tracer kinetics and pharmacokinetics in other animal models as well as in humans. While all these systems are widely accepted and have thus often been used for tracer modeling, they differ from the approach presented in this paper in mainly two ways. First, although the graphical modeling approaches are inherently visual, visualization does not play a major role in these systems. Second, the concurrent integration of multiple models and the ability to compare uncertainty of the output arisen during the process through visualization is not an integral part.

3. Kinetic PET Modeling

Kinetic PET modeling helps to isolate the components of interest from the obtained PET data. As a result, the analysis of the underlying mathematical model provides insight into the kinetic behavior of the tracer under investigation.

Kinetic PET modeling techniques may be divided into two groups: model-driven and data-driven methods. The model-driven techniques require a model structure as a-priori information (see Figure 1). In contrast data-driven algorithms obtain this information directly from the kinetic

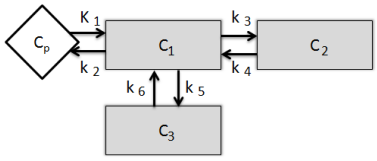

Figure 1: Three-tissue (or four-compartment) compartment model. This model consists of components of arterial plasma, $C_p(t)$, free ligand in tissue, $C_1(t)$, specific binding, $C_2(t)$, non-specific binding, $C_3(t)$, and six kinetic micro parameters, $K_1, k_2 \ldots, k_6$, describing the rate constants.

data, e. g., a dynamic PET (dPET) scan. Figure 1 shows a three-tissue (or four-compartment) compartment model. The first compartment, C_p, is the arterial blood. This compartment is also known as the input function. From the arterial blood, the radioligand passes into the second compartment, C_2, known as the free compartment. The third compartment, C_3, is the region of nonspecific-binding which we are usually interested to observe. The fourth compartment, C_4, is a nonspecific binding compartment that exchanges with the free compartment, C_1. $K_1, k_2 \ldots, k_6$ are the kinetic micro parameters describing the constant transfer rates between compartments. It is worth noting that K_1 is written in uppercase since it differs, with respect to several properties, from the other micro parameters, e. g., it is subject to a different measuring unit.

The following system of ordinary differential equations (ODEs) is the mathematical representation of the compartment model in Figure 1.

$$\begin{aligned} dC_1/dt &= K_1C_p(t)+k_5C_3(t)+k_4C_2(t)-(k_2+k_3+k_6)C_1(t) \\ dC_2/dt &= k_3C_1(t)-k_4C_2(t) \\ dC_3/dt &= k_6C_1(t)-k_5C_3(t) \end{aligned} \quad (1)$$

where $C_p(t)$, $C_1(t)$, $C_2(t)$, and $C_3(t)$ are radioactivity concentrations at time t for each compartment. It should be noted that a compartment model is always analyzed with respect to a region of interest (ROI) which could, in the most extreme cases, be the whole body or a single voxel inside an organ but is more often a single organ. When several organs are considered we refer to the model as a multi-level compartment model. Quantitative analysis of a compartment model is done through solving its mathematical representation. Depending on the given inputs different type of information can be obtained by solving the system of ODEs. For instance the mathematical prediction of the tissue activity (time-activity curve - TAC) can be obtained from a given input function, $C_p(t)$, and micro parameters. This is called the *forward* problem. On the other hand kinetic micro parameters can be estimated from a given input function, $C_p(t)$, and measured TACs. This is called the *backward* problem and can be solved by using different least squares fitting techniques such as linear least squares, nonlinear least squares, weighted integration [CHG86], generalized linear least squares [FHWH96] or basis function techniques [KHI85, CJ93, GLHC97]. In both cases the arterial

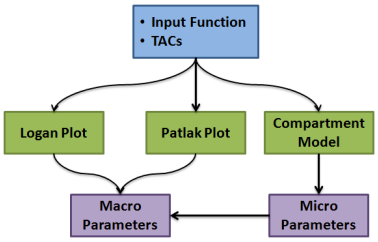

Figure 2: Dependency of the computed kinetic parameters. In a given ROI, based on the input function and the measured TACs, the macro parameter can be obtained directly from the Logan or the Patlak plot. The compartment modeling allows us to obtain micro parameters from which again macro parameters can be derived.

radioactivity concentration, $C_p(t)$, known as the input function must be provided. There are two approaches to obtain the input function: invasive and non-invasive methods. Although the non-invasive methods provide less accurate measurements, they are usually preferred [ZFCL*11]. Recent development of reference tissue models, e. g., [WCI00], however, help to avoid the blood sampling requirement.

Logan [Log00] plots and Patlak [PB85] plots are the two state-of-the-art data-driven modeling methods. These techniques employ a transformation of the data such that a linear regression of the transformed data yields the macro parameter of interest. Despite their inherent simplicity they can reliably provide good enough output. As a result, they are frequently used in practice. Nevertheless these techniques are biased due to statistical noise [SL00] and requires special handling when the resulting plot becomes non-linear. It should be noted that these macro parameters can also be derived from the micro parameters described above. For instance the net influx of the tracer obtained from the Patlak plot, K_i, can be derived from the micro parameters in the compartment model in Figure 1 as follows: $K_i = \frac{K_1 \times k_3}{k_2+k_3}$. In comparison with the micro parameters, macro parameters represent the observed data rather than the individual parameter. Spectral analysis [CJ93] is another data-driven modeling approach which characterizes the system impulse response function (IRF). In this approach the non-negative least square fitting is used, and the macro parameters are calculated as functions of the IRF. Although these techniques do not provide information about the underlying model structure, spectral analysis provides the number of tissue compartments evident in the data.

4. Deriving Intra- and Inter-Model Uncertainty

In this section we explain the variety of kinetic parameters computed and analyzed by our system, as well as the derivation of the associated intra- and inter-model uncertainty.

The dependency of modeling parameters is shown in Figure 2. Micro parameters can be estimated from the compartment model. Macro parameters can be obtained either by using the Logan or Patlak method or through the derivation from the micro parameters. These different sources of

macro parameters enable us to compute the inter-model uncertainty, while the covariance analysis can be used to derive intra-model uncertainty from the compartment model.

In the Patlak method the concentration of the tracer at time t after injection is described as follows

$$C(t) = \lambda \cdot C_p(t) + K_i \int_0^t C_p(\tau) d\tau \tag{2}$$

where $C(t)$ represents activity in the tissue as measured by the PET scanner, $C_p(t)$ is the plasma activity, K_i is the net rate of the tracer influx into the tissue, and λ is the distribution volume of the tracer. By dividing both sides of Equation 2 by $C_p(t)$, the macro parameter, K_i, can be estimated as the slope in the Patlak plot through the use of linear regression analysis. The Logan technique works in a similar fashion. For instance, the macro parameter which is the volume distribution of the tracer is obtained through a regression approach on the transformed data.

In compartmental modeling, micro parameters can be obtained by solving the system of ODEs. This is an optimization problem with the goal to minimize the weighted residual sum of squares (WRSS) defined as

$$\begin{aligned} \mathrm{WRSS}(\lambda) &= \sum_{j=1}^{N} w_i \left(C_{obs}(t_j) - C(t_j)\right)^2 \\ &= \sum_{j=1}^{N} w_i \left(C_{obs}(t_j) - e^{-\beta t_j}\right)^2 \end{aligned} \tag{3}$$

where β represents the kinetic parameters to be estimated, w_i is the weighting scheme, N is the number of measurements, and $C_{obs}(t_j)$ and $C(t_j)$ represent the measured data and the model prediction of the tracer activity at time t_j respectively. It is worth noting that the concentration of the tracer is a nonlinear function of the parameter β over time: $C(t_j) = e^{-\beta t_j}$. In order to calculate the associated uncertainty of the estimates of the kinetic parameters the bootstrap technique [TSB*98] is commonly used. This technique is, however, computational expensive. In this work we propose the analysis of the covariance matrix of the estimates to calculate the certainty level of the estimated kinetic parameters. In general the covariance matrix of the estimates of the kinetic parameters is symmetric. Particularly the diagonal elements are the variances of the parameter estimates which are positive by definition and the off-diagonal elements are the covariances which may be either positive or negative. Finding the optimal result from the minimization of the Equation 3 is an iterative process. During this process the information matrix constructed by the weighting scheme w_i, and the derivative of the function used to fit the data represents the minimum achievable covariance matrix as in Equation 4

$$Cov(\hat{p}) \geq M^{-1}(\hat{p}) \tag{4}$$

where $\hat{p}$ is the estimates of the kinetic parameters, $Cov(\hat{p})$ is the covariance matrix of the estimates, and M is the information matrix. The information matrix approaches the covariance matrix of the estimates for a large sample size of tissue

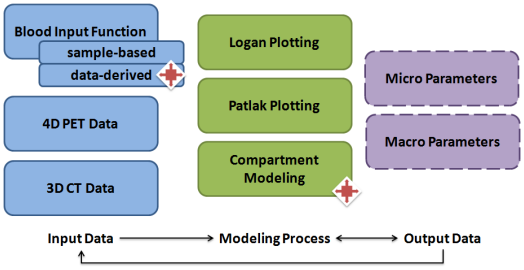

Figure 3: Workflow to derive the kinetic parameters and their associated uncertainties. Input data is fed into three different kinetic modeling techniques which are used to derive kinetic micro and macro parameters. These parameters are analyzed and the modeling uncertainty is derived based on the parameter variation. Thus the uncertain output data serves as a basis for changing model input parameters which can be interactively changed as depicted by the red arrows.

measurements and/or decreasing variance of the measurement error. Moreover the estimates also approach Gaussian distributions. It is worth noting that despite the fact that there are several sources of noise in PET imaging, the addition of these sources of errors tends to form a Gaussian distribution [ITY*98]. Thus, for an optimal weighted nonlinear least squares fitting, the covariance matrix of the estimates needs to reach the lower bound fined by the information matrix. As a result, the analysis of the covariance matrix of the estimates reveals the precision of the estimates which represents the intra-model uncertainty.

Since the macro parameters, obtained from either the Patlak plot or the Logan plot, represent the observed data rather than the individual parameters, the relative comparison between these values and the corresponding derivation from the micro parameters can provide useful information. We refer to the differences of macro parameters based on these three sources as inter-model uncertainty. For a thorough understanding of intra- and inter-model uncertainty, an appropriate visualization techniques is essential, which also allows for relating the intra-model uncertainty based on the micro parameters to the inter-model uncertainty based on the macro parameters.

5. Uncertainty-Aware Kinetic Parameter Visualization

We motivate the proposed visualization techniques by giving an overview of the underlying modeling workflow as illustrated in Figure 3. The three state-of-the-art kinetic PET modeling approaches, Logan plotting, Patlak plotting, and compartment modeling as are employed to provide the estimates of the kinetic parameters. By visually depicting the resulting intra- and inter-model uncertainty ranges we enable the user to modify the modifiable model input parameters (red arrows in Figure 3) with the goal to minimize the uncertainty and thus allow more realistic modeling results. It is worth mentioning that depending on the underlying problem solving approach, the parameters being modifiable may vary.

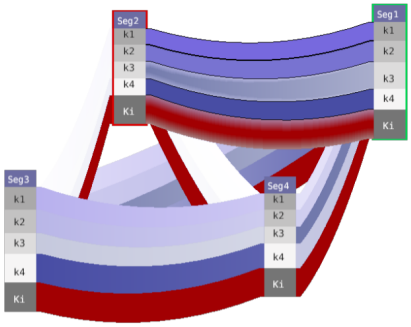

Figure 4: The uncertainty-aware visualization technique depicts differences in the micro and macro parameters. The color of the bands connecting the kinetic parameters between different ROIs is selected based on the pre-attentive process. Uncertainty is depicted by using blurring while certain values are emphasized through edge detections.

5.1. Kinetic Parameters Uncertainty Visualization

To be able to obtain more realistic modeling results it is essential to depict the modeling parameters as well as the intra- and the inter-model uncertainties. Therefore we propose an uncertainty-aware visualization technique as illustrated in Figure 4. The proposed visualization technique is based on the *ThemeRiver* metaphor [HHN00] which has been extended to visualize the parameter changes and the associated uncertainties dependent on spatial locations, i. e., micro and macro parameters together with the intra- and inter-model uncertainties computed for different ROIs. Each ROI is represented by a box that is subdivided based on the associated micro and macro parameters. Based on the connectivity in the underlying compartment model the boxes are connected through bands which depict changes in kinetic parameters as well as the associated uncertainty. The colors of these bands have been chosen to comply with the rules of pre-attentive perception [The92]. Initially macro parameters are in focus so they are colored in red, while the micro parameters, which are of interest in a later processing stage, are colored in shades of blue. To allow a better comparison of the micro and the macro parameters the bands are drawn such that the width of the curves is not affected by its curvature.

Besides the parameter changes the bands are also used to depict the uncertainties of the currently selected ROIs. We have chosen to keep the uncertainty depiction simple in order to reduce visual clutter. As the silhouette perception is an essential part of the shape perception process, silhouettes are a powerful mechanism in visual communication. Therefore in our case, to depict the underlying uncertainty we have decided to use parameter uncertainty as a modulation factor for dissolving or emphasizing the segments' shapes by blurring or edge enhancement. It should be noted that depending on the connected ROI representations, the uncertainty along a segment may vary. To realize various degrees of dissolution and emphasize, we combine blurring and edge detection techniques realized as post processing of the connection segments. When the uncertainty to be depicted is below the uncertainty threshold u_{min}, the regions of the segment are emphasized by adding a silhouette edge indicating certain values. All regions subject to an uncertainty exceeding u_{min} are vertically blurred based on the degree of uncertainty. We have to consider two things. First, the degree of blur needs to be based on the uncertainty, and second, the blurring should not affect the neighboring segment. To reach the first goal, we allow the user to define a maximum degree of blur specified through a maximal blur kernel size g_{max} as well as an upper uncertainty threshold u_{max}. Based on these values and the current uncertainty u, the kernel size g_{dim} for the Gaussian kernel used to achieve the desired effect can be derived by $g_{dim} = ((u - u_{min})/(u_{max} - u_{min})) \times g_{max}$. To reach the second goal, and avoid bleeding effects between adjacent segments, the Gaussian filter is adapted in such a way that for samples lying outside the current segment a desaturated version of the color of the current segment is used. Thus we are able to achieve effects as shown in Figure 6. It is worth noting that since the uncertainty information was not taken into account in the image on the left in Figure 6, the color is more saturated.

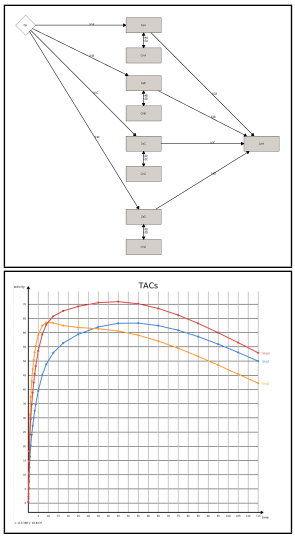

Figure 5: The compartment model (*left*) for three different organs can be considered as a state diagram, where the state changes over time. The TACs (*right*) are plotted over time after injection.

To depict the spatial position of the associated ROIs, the events originally connected along the time axis are now located in the image plane in a way that enables an easy association with the ROIs shown in the 3D view. Thus the layout of the boxes is associated with different ROIs in an associated 3D view (see Figure 7 (top left)). This association is important, as it shows how a tracer behaves in different organs and allows the domain expert to gain further insight into the kinetic behavior of the tracer under investigation.

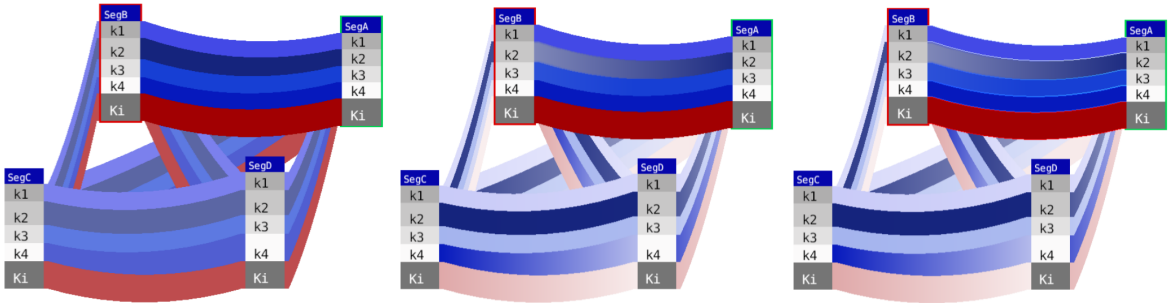

Figure 6: A high degree of uncertainty is depicted by using vertical blurring: no uncertainty depiction applied (*left*), uncertainty depiction without edge detection (*middle*) and uncertainty depiction with edge detection (*right*).

The proposed layout calculation algorithm contains two main steps and is executed whenever the ROI positions in the 3D view are changed, e. g., when the camera is rotated or zoomed. In the first step the ROI representations are positioned such that overlap is avoided and a direct mental linking with the original ROI positions in the 3D view can be established. In the second step we perform a relaxation of the position of the boxes in the horizontal and vertical direction, which maximizes the distances between these objects, and thus allows us to have sufficiently large connection between them. Thus, it improves the connectivity in the initial layout. The last step of the layout algorithm is performed in an animated manner and only when the user is not changing the positions of the ROIs in the 3D view. Thus we can ensure a coherent association with the ROI positions in the 3D view after the first step and a coherent transition to a layout optimized for the presented representation.

5.2. Linking Kinetic Parameters with Spatial and Temporal Attributes

While our uncertainty derivation and visualization methods provide further insights, they must be seen as an addition to previous visualization techniques and should be applied in a combined manner with these. As most of the data in the kinetic PET modeling process have both, spatial and temporal attributes, these properties need to be considered during the combination.

The TACs are, for instance, an abstract representation showing the tracer activity over time (see Figure 5 (right)). They are associated with a spatial position but are usually represented by a 2D plot, which has no spatial components. While the structure of the compartment model is usually presented in a 2D space, the compartment model itself inherently represents time through which the tracer transits between the compartments (see Figure 5 (left)). Moreover a compartment model is always associated with a spatial position given by the analyzed ROI. In contrast to the model structure the measured kinetic data given by the 4D PET is inherently spatial. Since PET is a rather low resolution modality, it suffers from partial volume effects. Thus PET is commonly fused with a co-registered CT scan to allow better spatial relations communication. As a result, the proposed integrated visualization combines these conventional 2D and 3D views to help users to relate the uncertainty, the TACs, and the model structure to their spatial anchor.

From the requirement analysis above we make use of the mental linking approach, which has shown to be a very useful when dealing with multiple visual representations in several application scenarios [Tor03, GRW*00, Dol07, BBP10, KVDG*10]. It is worth noting that linking in our case is more difficult since the analyzed data, e. g., 4D PET scans, is inherently spatial while the analysis techniques are primarily based on abstract representations, e. g., model structures and regression analysis plots.

Figure 7 illustrates the organization of the different views in an integrated visualization. The top left view is a multi-volume rendering view which has been enriched by depicting the ROIs through silhouette enhancement techniques. The view operates on three volumetric data sets: the PET data, the co-registered CT data used to provide the spatial context, and a segmentation volume which encodes the ROIs. Generation of this segmentation volume is not part of our system. The 3D view is linked to standard 2D

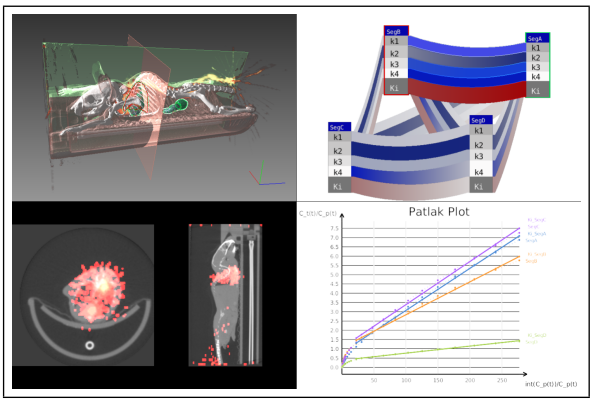

Figure 7: Our system employs multiple views supporting the kinetic modeling process. A multi-volume rendering view (*top left*) allows us to assess the spatial location of the input function sampling positions as well as of the ROIs. 2D slice views (*bottom left*) enable to assess tracer uptake in more detail and support repositioning of the image-derived input function sample locations. The plot (*bottom right*) shows the output of the Patlak graphical analysis. An uncertainty-aware widget (*top right*) reveals the modeling uncertainty.

slice representations arranged in the bottom left view. When the user scrolls through the shown slices, the slice indicators (green and red rectangle) in the 3D view are updated and indicate the current slice position. This allows an in-detail inspection of the relevant structures, while the 3D view provides an overview of the spatial context. These 2D views allow a better interaction when performing selection tasks when changing the image-derived input function locations is necessary. The output of the Logan/Patlak plot is shown on the bottom right.

6. Evaluation

To investigate the benefits of the proposed uncertainty-aware modeling concepts we have conducted an evaluation with three domain experts from the Turku PET Centre, which are working in nuclear medicine and conduct research related to kinetic PET modeling. The objective was to assess the users' ability to quickly perceive the uncertainty in the estimates of the kinetic parameters and derive meaningful information from the proposed visualizations.

In order to derive the uncertainty of the estimates we implemented a prototype software that supports compartmental modeling as shown in Figure 5. Spectral analysis is used to identify the initial number of compartments that are evident in the input data. The system also solves both the *forward* and the *backward* problems. In addition, the Patlak plotting and the Logan plotting techniques are also integrated.

We prepared four data sets containing different levels of synthetically introduced uncertainty into the ground-truth data, which lead to the different uncertainty in the estimates of the kinetic parameters. Figure 8 illustrates the uncertainty-aware visualization of two sets of kinetic parameters with different levels of uncertainty, whereby the uncertainty displayed in the ROI on the right is higher for all parameters. As it can be seen, color saturation and silhouette thickness vary dependent on the degree of uncertainty. We presented the visualizations of these four data sets to the three domain experts. While the ROIs on the left are subject to the same degree of uncertainty for each individual kinetic parameter, the ROIs on the right depict different sets of kinetic parameters with varying uncertainty. The participants were asked to perform the following tasks:

1. Organizing the visualizations in an increasing order of overall level of uncertainty in ROIs on the right.
2. Identifying the image in which the macro parameter K_i has the highest level of uncertainty.
3. Identifying the micro parameters that have the strongest influence on the uncertainty of the macro parameter K_i.

By using the proposed uncertainty-aware visualization technique all three participants could quickly perceive the underlying uncertainty of the kinetic parameters. In task 1, all the participants provided the correct increasing order of uncertainty level in ROIs on the right. We received one incorrect answer for the task 2. Particularly, the participant selected the image containing the second highest level of uncertainty. In task 3, the participants identified correctly the micro parameters that contribute most uncertainty to the derived macro parameter K_i. As we consider these results as very positive feedback, the proposed uncertainty-aware visualization technique seems to help to depict the uncertainty in the estimates of the kinetic parameters, while at the same time providing insights into the uncertainty contribution of the micro parameters to the derived macro parameter.

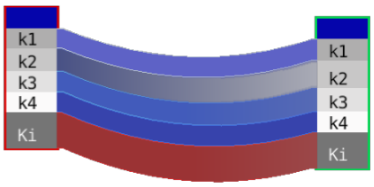

Figure 8: The uncertainty-aware visualization supports the relative uncertainty comparison between two different sets of kinetic parameters.

Apart from the task results, we also received very positive comments from the domain experts. Among them the statement, that the proposed visualization technique enables to identify the uncertainty contribution of the micro parameters to the derived macro parameters, which is not possible with the standard bar plot used to depict the kinetic parameters. One domain expert also requested more information about the software and its availability.

When querying feedback regarding the uncertainty derivation approach the domain experts stated that the proposed uncertainty derivation approach is comparable to the commonly used bootstrap technique. As the bootstrap technique is a statistical approach, the analysis of the covariance matrix is a viable alternative. Since the analysis of the covariance matrix is done with an iterative weighted nonlinear least squares fitting, it requires less computation than the bootstrap approach.

7. Conclusions and Future Work

In this paper we have presented another approach to the derivation of uncertainty in the standard kinetic PET modeling. By combining the results of different state-of-the-art PET modeling techniques, e. g., Logan plots, Patlak plots and compartment modeling, together with sample-based and data-derived input functions, we are able to compute intra- and inter-model uncertainties for kinetic modeling parameters. To communicate the parameters and their associated uncertainty a novel uncertainty-aware visualization technique was proposed and incorporated into an integrated visualization. While the uncertainty-aware visualization allows the user to estimate the differences in the model output, the interactive visual feedback in the integrated visualization enables to adapt the input parameters in order to minimize the uncertainty. Furthermore the linked views in the integrated visualization also depict both the spatial and temporal nature of the kinetic data to assist the kinetic PET modeling process.

There are several interesting research opportunities for the

future. While the uncertainty-aware visualization technique enables users to compare the uncertainty in the estimates of the kinetic parameters, the combination with a machine learning techniques to assist the uncertainty reduction process is an interesting research direction. It could be possible to allow a semi-automatic uncertainty reduction based on the interplay between human and computer. Furthermore the integration of histological findings into the proposed integrated visualization approach would be an interesting next step towards more effective kinetic PET modeling.

Acknowledgments

We gratefully acknowledge the feedback and the evaluation from Vesa Oikonen and his colleagues from Turku PET Center, University of Turku.

References

[AMM*08] AIGNER W., MIKSCH S., MULLER W., SCHUMANN H., TOMINSKI C.: Visual methods for analyzing time-oriented data. *IEEE Transactions on Visualization and Computer Graphics 14*, 1 (2008), 47 –60. 2

[BB97] BURGER C., BUCK A.: Requirements and implementation of a flexible kinetic modeling tool. *Journal of Nuclear Medicine 38*, 11 (1997), 1818. 1, 2

[BBC*98] BARRETT P., BELL B., COBELLI C., GOLDE H., SCHUMITZKY A., VICINI P., FOSTER D.: SAAM II: simulation, analysis, and modeling software for tracer and pharmacokinetic studies. *Metabolism Clinical and Experimental 47*, 4 (1998), 484–492. 1, 2

[BBP10] BUSKING S., BOTHA C., POST F.: Dynamic multi-view exploration of shape spaces. In *Computer Graphics Forum* (2010), vol. 29, Wiley Online Library, pp. 973–982. 6

[BVG10] BALABANIAN J., VIOLA I., GRÖLLER E.: Interactive illustrative visualization of hierarchical volume data. In *Proceedings of Graphics Interface* (2010), Canadian Information Processing Society, pp. 137–144. 2

[BYV*08] BALABANIAN J.-P., YSTAD M., VIOLA I., LUNDERVOLD A., HAUSER H., GRÖLLER M. E.: Hierarchical volume visualization of brain anatomy. In *Proceeding of Vision, Modeling and Visualization (VMV 2008)* (2008), pp. 313–322. 2

[CHG86] CARSON R., HUANG S., GREEN M.: Weighted integration method for local cerebral blood flow measurements with positron emission tomography. *Journal of Cerebral Blood Flow & Metabolism 6*, 2 (1986), 245–258. 3

[CHP81] CARSON R., HUANG S., PHELPS M.: BLD: a software system for physiological data handling and model analysis. In *Proceedings of the Annual Symposium on Computer Application in Medical Care* (1981), American Medical Informatics Association, p. 562. 1, 2

[CJ93] CUNNINGHAM V., JONES T.: Spectral analysis of dynamic pet studies. *Journal of Cerebral Blood Flow & Metabolism 13*, 1 (1993), 15–23. 3

[Dol07] DOLEISCH H.: SimVis: Interactive visual analysis of large and time-dependent 3D simulation data. In *Simulation Conference, 2007 Winter* (2007), IEEE, pp. 712–720. 6

[FHWH96] FENG D., HUANG S., WANG Z., HO D.: An unbiased parametric imaging algorithm for nonuniformly sampled biomedical system parameter estimation. *IEEE Transactions on Medical Imaging 15*, 4 (1996), 512–518. 3

[GLHC97] GUNN R., LAMMERTSMA A., HUME S., CUNNINGHAM V.: Parametric imaging of ligand-receptor binding in pet using a simplified reference region model. *Neuroimage 6*, 4 (1997), 279–287. 3

[GRW*00] GRESH D., ROGOWITZ B., WINSLOW R., SCOLLAN D., YUNG C.: WEAVE: A system for visually linking 3-D and statistical visualizations, applied to cardiac simulation and measurement data. In *Proceedings of the conference on Visualization* (2000), IEEE, pp. 489–492. 6

[HHN00] HAVRE S., HETZLER B., NOWELL L.: Themeriver: visualizing theme changes over time. In *IEEE Symposium on Information Visualization* (2000), pp. 115–123. 1, 2, 5

[HLX11] HUAIQING H., LEI Y., XU Q.: Multidimensional uncertainty visualization with parallel coordinate and star glyph. *International Journal of Digital Content Technology and its Applications 5*, 6 (2011), 412–420. 2

[HTW*05] HUANG S., TRUONG D., WU H., CHATZIIOANNOU A., SHAO W., WU A., PHELPS M.: An internet-based kinetic imaging system (KIS) for MicroPET. *Molecular Imaging and Biology 7*, 5 (2005), 330–341. 2

[Ins85] INSELBERG A.: The plane with parallel coordinates. *The Visual Computer 1*, 2 (1985), 69–91. 2

[ITY*98] IKOMA Y., TOYAMA H., YAMADA T., UEMURA K., KIMURA Y., SENDA M., UCHIYAMA A.: Creation of a dynamic digital phantom and its application to a kinetic analysis]. *Kaku igaku. The Japanese journal of nuclear medicine 35*, 5 (1998), 293. 4

[JS03] JOHNSON C., SANDERSON A.: A next step: Visualizing errors and uncertainty. *IEEE Computer Graphics and Applications 23*, 5 (2003), 6–10. 2

[KHI85] KOEPPE R., HOLDEN J., IP W.: Performance comparison of parameter estimation techniques for the quantitation of local cerebral blood flow by dynamic positron computed tomography. *Journal of Cerebral Blood Flow & Metabolism 5*, 2 (1985), 224–234. 3

[KVDG*10] KREKEL P., VALSTAR E., DE GROOT J., POST F., NELISSEN R., BOTHA C.: Visual analysis of multi-joint kinematic data. In *Computer Graphics Forum* (2010), vol. 29, Wiley Online Library, pp. 1123–1132. 6

[Log00] LOGAN J.: Graphical analysis of pet data applied to reversible and irreversible tracers. *Nuclear medicine and biology 27*, 7 (2000), 661–670. 3

[MC01] MUZIC R., CORNELIUS S.: Comkat: compartment model kinetic analysis tool. *Journal of Nuclear Medicine 42*, 4 (2001), 636. 1, 2

[MMHE11] MALIK A., MACIEJEWSKI R., HODGESS E., EBERT D.: Describing temporal correlation spatially in a visual analytics environment. In *Hawaii International Conference on System Sciences* (2011), pp. 1 –8. 2

[ODH*07] OELTZE S., DOLEISCH H., HAUSER H., MUIGG P., PREIM B.: Interactive visual analysis of perfusion data. *IEEE Transactions on Visualization and Computer Graphics 13*, 6 (2007), 1392–1399. 2

[PB85] PATLAK C., BLASBERG R.: Graphical evaluation of blood-to-brain transfer constants from multiple-time uptake data. generalizations. *Journal of Cerebral Blood Flow & Metabolism 5*, 4 (1985), 584–590. 3

[PWL97] PANG A., WITTENBRINK C., LODHA S.: Approaches to uncertainty visualization. *The Visual Computer 13*, 8 (1997), 370–390. 2

[SL00] SLIFSTEIN M., LARUELLE M.: Effects of statistical noise on graphic analysis of pet neuroreceptor studies. *Journal of Nuclear Medicine 41*, 12 (2000), 2083. 3

[The92] THEEUWES J.: Perceptual selectivity for color and form. *Attention, Perception, & Psychophysics 51*, 6 (1992), 599–606. 5

[Tor03] TORY M.: Mental registration of 2D and 3D visualizations (an empirical study). In *IEEE Visualization* (2003), pp. 371–378. 6

[TSB*98] TURKHEIMER F., SOKOLOFF L., BERTOLDO A., LUCIGNANI G., REIVICH M., JAGGI J., SCHMIDT K.: Estimation of component and parameter distributions in spectral analysis. *Journal of Cerebral Blood Flow & Metabolism 18*, 11 (1998), 1211–1222. 4

[Wal04] WALKER D.: The use of pharmacokinetic and pharmacodynamic data in the assessment of drug safety in early drug development. *British journal of clinical pharmacology 58*, 6 (2004), 601–608. 1

[WCI00] WATABE H., CARSON R., IIDA H.: The reference tissue model: Three compartments for the reference region. *NeuroImage 11*, 6 (2000), S12. 3

[ZFCL*11] ZANOTTI-FREGONARA P., CHEN K., LIOW J., FUJITA M., INNIS R.: Image-derived input function for brain pet studies: many challenges and few opportunities. *Journal of Cerebral Blood Flow & Metabolism* (2011). 3